

UrQMD simulations of higher-order cumulants in Au+Au collisions at high baryon density

Xin Zhang (张鑫)^{1,2†} Yu Zhang (张宇)³ Xiaofeng Luo (罗晓峰)⁴ Nu Xu (许怒)^{1,4‡}

¹Institute of Modern Physics, Chinese Academy of Sciences, Lanzhou 730000, China

²School of Nuclear Science and Technology, University of Chinese Academy of Sciences, Beijing 100049, China

³School of Physics and Technology, Guangxi Normal University, Guilin 541001, China

⁴Key Laboratory of Quark and Lepton Physics (MOE) and Institute of Particle Physics, Central China Normal University, Wuhan 430079, China

Abstract: High moments of conserved quantities, such as net-baryon, net-electric charge, and net-strangeness, in heavy-ion collisions are sensitive to fluctuations caused by the quantum chromodynamics critical point (CP). The event-by-event analysis of high moments of the conserved charges has been widely used in experiments to search for the CP, particularly in the RHIC-STAR experiment. To establish a *dynamical non-critical baseline*, particularly in the high baryon density region, we performed a systematic analysis of the proton multiplicity distributions from Au+Au collisions at $3 \leq \sqrt{s_{NN}} \leq 9.2$ GeV. The beam energy, centrality, and rapidity width dependence of proton (factorial) cumulants, up to the 4th order, were extracted from the calculations of a hadronic transport model called the ultra-relativistic quantum molecular dynamics (UrQMD) model. In addition, the effects of the initial volume fluctuation are discussed. These results will be important for the physics analysis of the RHIC Beam Energy Scan (BES) data, particularly for the fixed-target data and experimental data from future CBM experiments at FAIR.

Keywords: QCD critical point, heavy-ion collisions, proton (factorial) cumulants, initial volume fluctuation, dynamical non-critical baseline

DOI: 10.1088/1674-1137/ae0995 **CSTR:** 32044.14.ChinesePhysicsC.50011003

I. INTRODUCTION

The main task of heavy-ion collision experiments is to study the properties of quark-gluon plasma and the phase structure of strongly interacting matter, which can be displayed by a quantum chromodynamics (QCD) phase diagram in terms of temperature T and baryon chemical potential (μ_B). Recently, theoretical studies have predicted a QCD critical point (CP) at the end of the first-order phase transition boundary, but there is no consensus on the theoretical side on the exact location of the CP [1–8].

On the experimental side, in the search for the QCD CP, higher-order cumulants of conserved quantities, such as net-baryon, net-strangeness, and net-electric charge, are proposed as promising observables owing to their sensitivity to system correlation length ξ , which tends to diverge at around the CP [9–12]. The Beam Energy Scan program at the BNL Relativistic Heavy Ion Collider (RHIC) by the STAR experiment has collected large datasets over a wide range of collision energies $\sqrt{s_{NN}} = 7.7–200$ GeV of Au+Au collisions. Assuming that the thermalization is reached in those collisions, the corre-

sponding range of chemical potential is $\mu_B \sim 420–? 25$ MeV. The STAR experiment has published a series of papers on high moments related to the QCD CP [13–25]. Recent STAR results on the net-proton C_4/C_2 [18, 19, 26] have shown a non-monotonic energy dependence trend with a significance level of 3.1σ , which could be a signature of the QCD CP. The subsequent net-proton analysis on BES-II datasets ($\sqrt{s_{NN}} = 7.7–27$ GeV), which have 10 to 20 times larger statistics, has significantly reduced statistical uncertainties [27]. During the second phase of the Beam Energy Scan, BES-II, STAR also obtained data in fixed-target mode (FXT) and collected Au+Au collision data at $\sqrt{s_{NN}} = 3.0–4.5$ GeV for proton high-moment analysis. The FXT data extended the QCD CP search to an unprecedented high baryon density region, where $\mu_B \sim 750$ MeV. The first publication of the proton high moments of STAR fixed-target data in Au+Au collisions at $\sqrt{s_{NN}} = 3.0$ GeV shows the consistency between data and hadronic transport model calculation, indicating that the CP could exist only at energies higher than 3.0 GeV [21, 22]. Measurements in the baryon density region will be crucial to establish a complete energy dependence trend.

Received 10 July 2025; Accepted 19 September 2025; Accepted manuscript online 20 September 2025

[†] E-mail: zhangxin205@mailsucas.ac.cn

[‡] E-mail: nxu@impcas.ac.cn

©2026 Chinese Physical Society and the Institute of High Energy Physics of the Chinese Academy of Sciences and the Institute of Modern Physics of the Chinese Academy of Sciences and IOP Publishing Ltd. All rights, including for text and data mining, AI training, and similar technologies, are reserved.

There have been several publications of non-critical model calculations [28] as baselines for net-proton high moment measurement, whereas those in the high baryon density region are scarce. As noted in Refs. [22], fluctuation analysis suffers from the so-called initial volume fluctuation effect. The effect emerges in experimental measurements when using charged particle multiplicity as a reference for collision centrality. From the experimental side, one could estimate the initial volume fluctuation effect by evaluating the centrality resolution of reference multiplicity at a certain energy. Generally, limited reference multiplicity indicates low centrality resolution, which brings a large initial volume effect into high moment measurements, particularly for higher-order ones.

In this paper, we show (net-)proton moment calculations using a hadronic transport model called the ultra-relativistic quantum molecular dynamics (UrQMD) model for Au+Au collisions at $\sqrt{s_{NN}} = 3.0\text{--}9.2$ GeV and discuss the effect of the initial volume fluctuation on high moments. In Sec. II, we briefly introduce the UrQMD model and simulation setup, as well as calculation details. In Sec. III, we show the model results and compare them with experimental data. We provide a summary in Sec. IV.

II. URQMD MODEL AND CALCULATION DETAILS

A. UrQMD model

The UrQMD model [29, 30] is a hadronic transport model successfully used in simulating (ultra-)relativistic heavy-ion collisions at a wide range of energies from SIS to RHIC. In UrQMD, hadrons have explicit space-time evolution trajectories. Below $\sqrt{s_{NN}} = 5$ GeV, particle production is described by interactions between hadrons and resonances, and at collision energies above $\sqrt{s_{NN}} = 5$ GeV, the excitation of color strings and their fragmentation into hadrons dominate particle production.

In this study, we simulate Au+Au collisions at $\sqrt{s_{NN}} = 3.0\text{--}9.2$ GeV in the UrQMD model configured in the standard cascade mode. The impact parameter (b) is set to 0 to 16 fm. The statistics at each energy are shown in Table 1.

B. Analysis details

The cumulants of a distribution up to the fourth order are defined as follows:

$$\begin{aligned} C_1 &= \langle N \rangle, & C_2 &= \langle (\delta N)^2 \rangle, \\ C_3 &= \langle (\delta N)^3 \rangle, & C_4 &= \langle (\delta N)^4 \rangle - 3\langle (\delta N)^2 \rangle^2, \end{aligned} \quad (1)$$

where N is the number of protons in each event, and $\delta N = N - \langle N \rangle$ is the deviation from the mean value $\langle N \rangle$. Cumulant ratios, such as C_2/C_1 , C_3/C_2 , and C_4/C_2 , are used to cancel volume dependence and are shown below:

$$\frac{C_2}{C_1} = \sigma^2/M, \quad \frac{C_3}{C_2} = S\sigma, \quad \frac{C_4}{C_2} = \kappa\sigma^2 \quad (2)$$

where M , σ^2 , S , and κ represent the mean value, variance, skewness, and kurtosis, respectively. Higher-order cumulants, such as skewness and kurtosis, are famous for their capability to measure non-Gaussianity. The factorial cumulants (κ_n) are related to the corresponding cumulants through the following relations:

$$\begin{aligned} \kappa_1 &= C_1 = \langle N \rangle, \\ \kappa_2 &= -C_1 + C_2, \\ \kappa_3 &= 2C_1 - 3C_2 + C_3, \\ \kappa_4 &= -6C_1 + 11C_2 - 6C_3 + C_4 \end{aligned} \quad (3)$$

In this study, the calculations of proton and net-proton high moments follow the same procedure used in experimental data analysis. Collision centrality is determined using charged particle multiplicity, including π^\pm and K^\pm . To approximate the acceptance of the STAR Au+Au collision experiment at each energy (3–9.2 GeV), π^\pm and K^\pm are counted within $-2.0 < \eta < 0$ for 3.0 GeV, $-2.4 < \eta < 0$ for 3.2–4.9 GeV, and $|\eta| < 1.6$ for 7.7 and 9.2 GeV. Protons and anti-protons are not included in the multiplicity definition to avoid self-correlation [31, 32]. The formation of light fragments, such as deuterons, is not included in the UrQMD calculation. As shown in previous studies [33, 34], deuterons and other light nuclei are formed via the coalescence of nearby protons and neutrons, which effectively removes correlated protons from the free nucleon sample and leads to an increase in the proton cumulant ratios. As discussed in [35], the effect of deuteron formation is similar to the binomial efficiency effect owing to the loss of protons via deuteron formation. The formation of light fragments should be considered when comparing with data.

Figure 1 shows the charged particle multiplicity distributions in Au+Au collisions at $\sqrt{s_{NN}} = 3.0\text{--}9.2$ GeV in

Table 1. Statistics of Au+Au collisions simulated in the UrQMD model at $\sqrt{s_{NN}} = 3.0\text{--}9.2$ GeV.

$\sqrt{s_{NN}}/\text{GeV}$	3.0	3.2	3.5	3.9	4.5	4.9	7.7	9.2
Events (million)	66	117	131	105	93	136	170	156

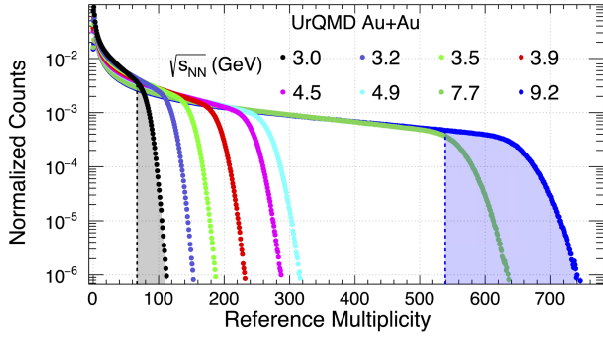


Fig. 1. (color online) Reference multiplicity distribution in Au+Au collisions at $\sqrt{s_{NN}} = 3.0, 3.2, 3.5, 3.9, 4.5, 4.9, 7.7,$ and 9.2 GeV calculated using the UrQMD model. The black and blue shaded regions indicate the most central 0%–5% collisions.

the UrQMD model. The charged particle multiplicity distribution is then fitted by the Monte Carlo Glauber model [36], and categorized into several centrality classes: 0%–5%, 5%–10%, ..., 70%–80%. The black and blue shaded regions in Fig. 1 indicate the 0%–5% collision centrality class. The centrality bin width correction method [31] is used in proton and net-proton cumulant calculation. Cumulants are calculated in each reference multiplicity bin, and then, the weighted average for each centrality bin is calculated. The statistical errors are determined via analytical equations using the Delta method [37].

Figure 2 shows the proton acceptance in transverse momentum (p_T) versus proton rapidity (y) in the center-of-mass frame in Au+Au collisions at $\sqrt{s_{NN}} = 3.0$ and 4.9 GeV from the UrQMD model. The black and red boxes indicate analysis windows within $0.4 < p_T < 2.0$ GeV/c and $-0.5 < y < 0$ and $|y| < 0.5$, respectively.

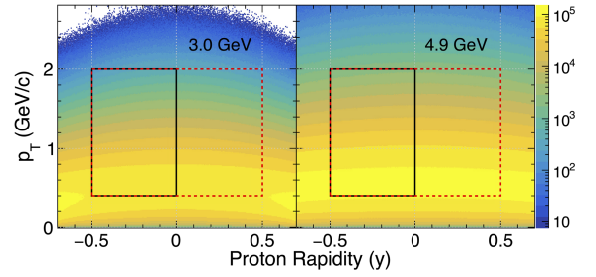


Fig. 2. (color online) Transverse momentum (p_T) versus proton rapidity (y) in Au+Au minimum bias collisions at $\sqrt{s_{NN}} = 3.0$ and 4.9 GeV calculated using the UrQMD model. Protons at rapidity $|y| < 0.5$ (red-dashed box) and $-0.5 < y < 0.0$ (black box) are used in the analysis for the collider and FXT mode, respectively.

III. RESULTS AND DISCUSSION

In this section, we show the calculations of proton and net-proton cumulant ratios in the UrQMD model.

Figure 3 shows the centrality dependence of proton cumulant ratio C_4/C_2 in Au+Au collisions at $\sqrt{s_{NN}} = 3.0$ – 9.2 GeV calculated using the UrQMD model. The dashed line at unity indicates a baseline from Poisson distribution. In mid-central and peripheral collisions, the proton ratio C_4/C_2 largely deviates from the Poisson baseline, which demonstrates the poor centrality resolution of the reference multiplicity, particularly at lower energies. The proton ratio C_4/C_2 shown with black dots is closer to the Poisson baseline than the results denoted by red squares, as the narrower proton distribution with $-0.5 < y < 0$ converges to the Poisson statistic rather than a wider distribution selected by $|y| < 0.5$.

As shown in the figure, the proton high moments, $\kappa\sigma^2$, have been suppressed in both central and peripheral collisions, particularly at the lowest collision energy

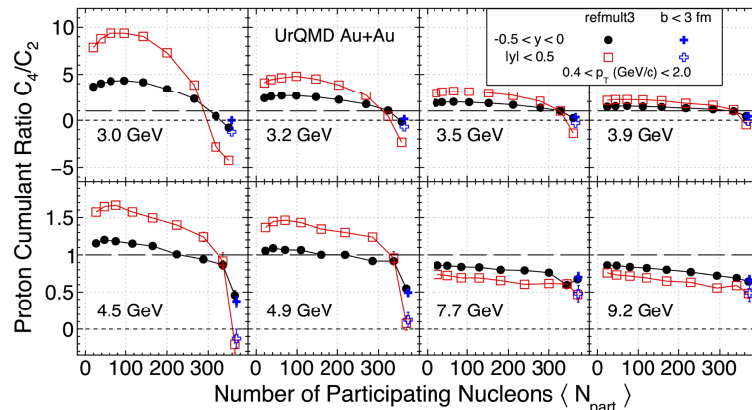


Fig. 3. (color online) Centrality dependence of the proton cumulant ratio, C_4/C_2 , in Au+Au collisions at $\sqrt{s_{NN}} = 3.0$ – 9.2 GeV calculated using the UrQMD model. The solid black circles and red open squares represent the results for protons at rapidity acceptance $-0.5 < y < 0$ and $|y| < 0.5$, respectively. The blue solid crosses and open crosses indicate calculations with a cut on the impact parameter $b \leq 3$ fm, for $-0.5 < y < 0$ and $|y| < 0.5$, respectively. For these calculations, the p_T acceptance of protons and anti-protons is $0.4 < p_T < 2.0$ GeV/c.

$\sqrt{s_{NN}} = 3.0$ GeV. The observed suppression decreases with increasing collision energy, and is more pronounced for the wider rapidity $|y| < 0.5$. In addition, the largest fluctuation from unity is observed in the mid-central collisions $\langle N_{\text{part}} \rangle \sim 100$. The negative value of the ratios is caused by the initial volume fluctuation; see the discussion below. The suppression at the most central collisions is due to the fixed number of incoming nucleons.

Now, let us focus on the results from the most central collisions: for protons from rapidity $|y| < 0.5$, the values of C_4/C_2 ratios are negative until the collision energy reaches 4.9 GeV, and this is true even for events selected from the cuts by the impact parameter b as shown by the open- and filled-blue crosses in the figure. For collision energy $\sqrt{s_{NN}} > 4.5$ GeV, all the ratios become positive, the values of the ratios from wider rapidity bins become smaller than those from the narrower bin $-0.5 < y < 0$, and they decrease from peripheral to central collisions. These results indicate the diminishing role of the initial volume fluctuations and baryon number conservations in such collisions.

Figure 4 shows the correlation distribution of the reference multiplicity vs. N_{part} and b vs. N_{part} in Au+Au collisions at $\sqrt{s_{NN}} = 3.0$ GeV, calculated using the UrQMD model. The vertical black dashed line indicates the 0%–5% central collisions selected by the reference multiplicity, and the vertical red dashed line indicates a cut on $b \leq 3$ fm. One can compare these two cuts on the N_{part} distributions. The $\langle N_{\text{part}} \rangle$ determined by the reference multiplicity, as in the experiment, shows a much wider

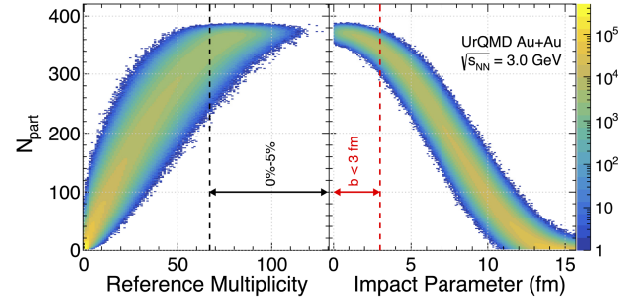


Fig. 4. (color online) Left panel: Correlation distribution of reference multiplicity vs. N_{part} in Au+Au collisions at $\sqrt{s_{NN}} = 3.0$ GeV calculated using the UrQMD model. The vertical black dashed line indicates the 0%–5% central collisions selected by the reference multiplicity. Right panel: Correlation distribution of b vs. N_{part} . The vertical red dashed line indicates a cut on $b \leq 3$ fm.

variation in the N_{part} distribution (see the left plot), compared with that of the $\langle N_{\text{part}} \rangle$ extracted from the cut on the impact parameter $b \leq 3$ fm (see the right plot). Conversely, for a fixed range of the N_{part} distribution, a much wider fluctuation is observed in the "measured" reference multiplicity compared with the impact parameter. The variations in the N_{part} distribution are the root cause of the initial volume fluctuations shown in Fig. 3. Note that such variation is part of the collision dynamics, and it should be properly simulated in the physics analysis.

Figure 5 shows the proton cumulant ratios C_2/C_1 , C_3/C_2 , and C_4/C_2 (left panels) and factorial cumulant ratios κ_2/κ_1 , κ_3/κ_1 , and κ_4/κ_1 (right panels) as a function of

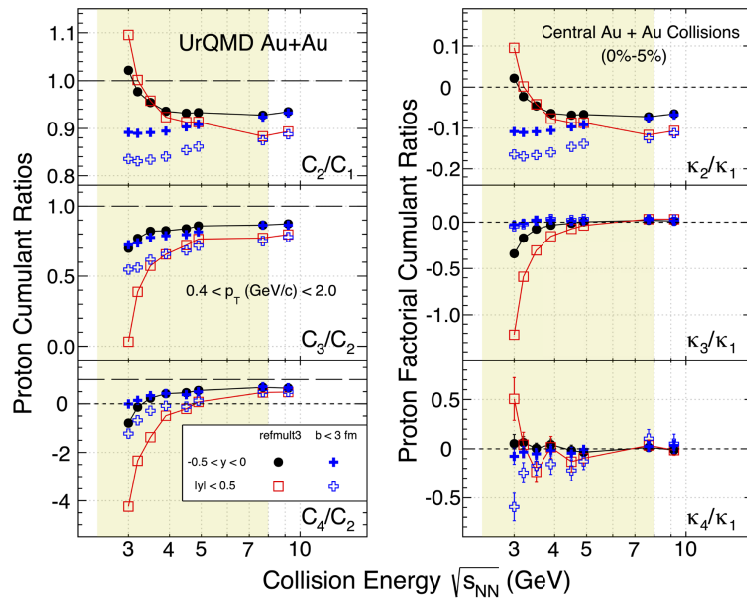


Fig. 5. (color online) Collision energy dependence of proton cumulant ratios (C_2/C_1 , C_3/C_2 , and C_4/C_2) and factorial cumulant ratios (κ_2/κ_1 , κ_3/κ_1 , and κ_4/κ_1) in 0%–5% central Au+Au collisions from the UrQMD model. The black solid circles and red open squares represent proton results at rapidity acceptance $-0.5 < y < 0$ and $|y| < 0.5$, respectively. The blue solid crosses and open crosses represent calculations with a cut on $b \leq 3$ fm, for $-0.5 < y < 0$ and $|y| < 0.5$, respectively.

collision energy in central collisions 0%–5% within kinematic acceptance $0.4 < p_T < 2.0$ GeV/c. The results of $b \leq 3$ fm are shown as solid crosses ($-0.5 < y < 0$) and open crosses ($|y| < 0.5$). As mentioned in the previous paragraph, the large difference between the reference multiplicity 0%–5% and $b \leq 3$ fm is mainly caused by the initial volume fluctuations. As the collision energy increases, while the ratios C_3/C_2 , C_4/C_2 , and κ_3/κ_1 show an initial fast increase and saturation at energies above 5 GeV, the ratios C_2/C_1 and κ_2/κ_1 behave in the opposite way. In any case, protons from wider rapidity bins show more sensitivity to the initial volume fluctuation, particularly in the high baryon density region.

Figure 6 shows the collision energy dependence of the proton and net-proton C_4/C_2 ratios from 0%–5% central collisions. The experimental measurements in $\sqrt{s_{NN}} = 7.7$ –19.6 GeV Au+Au collisions from RHIC-STAR BES-II data are also shown as red solid circles [18] from collider collisions, and the 3 GeV results are denoted by blue squares. The results of the UrQMD model calculations are displayed as colored bands: protons from $-0.5 < y < 0$ and net-protons from $|y| < 0.5$ are presented as blue and red bands, respectively. In both cases, both bands decreased as the collision energy decreased owing to both baryon number conservation and volume fluctuations. Owing to large acceptance in the case of the net-protons from $|y| < 0.5$, the decreases in the C_4/C_2 ratio are much faster in the low energy region. While there was a large deviation between data and the UrQMD model calculation at 19.6 GeV, the transport model well reproduced the data at $\sqrt{s_{NN}} = 3$ GeV. The result indicates that, if the CP exists, it should be between $3 < \sqrt{s_{NN}} < 19.6$ GeV Au+Au collisions. In addition to the Beam Energy Scan program at RHIC, the physics program at the Facility for Antiproton and Ion Research (FAIR) via the Compressed Baryonic Matter (CBM) experiment [38] is essential to finally determine the location of the QCD CP.

IV. SUMMARY

We present the results of proton (from $-0.5 < y < 0$)

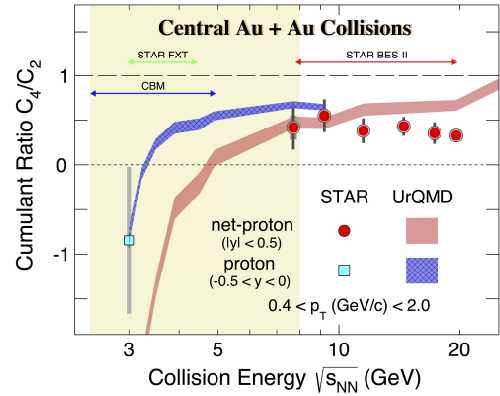


Fig. 6. (color online) Collision energy dependence of proton and net-proton cumulant ratio, C_4/C_2 , in 0%–5% central Au+Au collisions from the UrQMD model. The blue and red bands represent proton and net-proton results in UrQMD, respectively. The red and cyan markers represent STAR measurements from BES-II and the fixed-target experiment, respectively. In addition, the green and blue arrows indicate the collision energy range of the STAR fixed-target experiment at RHIC and the CBM experiment at FAIR, respectively.

and net-proton (from $|y| < 0.5$) high order cumulant ratios in Au+Au collisions at $\sqrt{s_{NN}} = 3.0$ –19.6 GeV obtained from calculations using the UrQMD model (hadronic transport model). These results are valuable dynamic references for the QCD CP search, and there are two main observations from these analyses. (i) At low energy $\sqrt{s_{NN}} < 5$ GeV, the initial volume fluctuation is important; the larger the acceptance, the stronger the effect of the fluctuation. (ii) In the FXT Au+Au collisions below $\sqrt{s_{NN}} < 5$ GeV, the UrQMD model calculations well reproduced the C_4/C_2 ratios, indicating that, if the QCD CP exists, it should be in the energy range $\sqrt{s_{NN}} > 3.0$ GeV.

Recently, the preliminary results of the proton cumulant in the RHIC-STAR fixed-target experiment at $\sqrt{s_{NN}} = 3.2$ –3.9 GeV have been reported [39]. The future CBM experiment at the FAIR [38] will consider a collision energy of $\sqrt{s_{NN}} = 2.4$ –4.9 GeV, with excellent acceptance and higher statistics to reduce both statistical and systematic uncertainties, and will play an important role in the QCD CP search.

References

- [1] D. A. Clarke, P. Dimopoulos, F. Di Renzo *et al.*, (2024), arXiv: 2405.10196[hep-lat]
- [2] G. Basar, *Phys. Rev. C* **110**, 015203 (2024), arXiv: 2312.06952[hep-th]
- [3] M. Hippert, J. Grefa, T. A. Manning *et al.*, *Phys. Rev. D* **110**, 094006 (2024), arXiv: 2309.00579[nucl-th]
- [4] W.-j. Fu, J. M. Pawłowski, and F. Rennecke, *Phys. Rev. D* **101**, 054032 (2020), arXiv: 1909.02991[hep-ph]
- [5] P. J. Gunkel and C. S. Fischer, *Phys. Rev. D* **104**, 054022 (2021), arXiv: 2106.08356[hep-ph]
- [6] F. Gao and J. M. Pawłowski, *Phys. Lett. B* **820**, 136584 (2021), arXiv: 2010.13705[hep-ph]
- [7] A. Sorensen and P. Sorensen, (2024), arXiv: 2405.10278[nucl-th]
- [8] H. Shah, M. Hippert, J. Noronha *et al.*, (2024), arXiv: 2410.16206[hep-ph]
- [9] Y. Hatta and M. A. Stephanov, *Phys. Rev. Lett.* **91**, 102003 (2003) [Erratum: *Phys. Rev. Lett.* **91**, 129901 (2003)], arXiv: hep-ph/0302002
- [10] M. Asakawa and M. Kitazawa, *Prog. Part. Nucl. Phys.* **90**,

- 299 (2016), arXiv: 1512.05038[nucl-th]
- [11] M. Kitazawa and X. Luo, *Phys. Rev. C* **96**, 024910 (2017), arXiv: 1704.04909[nucl-th]
- [12] X. Luo and N. Xu, *Nucl. Sci. Tech.* **28**, 112 (2017), arXiv: 1701.02105[nucl-ex]
- [13] M. M. Aggarwal *et al.* (STAR), *Phys. Rev. Lett.* **105**, 022302 (2010), arXiv: 1004.4959[nucl-ex]
- [14] L. Adamczyk *et al.* (STAR), *Phys. Rev. Lett.* **112**, 032302 (2014), arXiv: 1309.5681[nucl-ex]
- [15] L. Adamczyk *et al.* (STAR), *Phys. Rev. Lett.* **113**, 092301 (2014), arXiv: 1402.1558[nucl-ex]
- [16] L. Adamczyk *et al.* (STAR), *Phys. Lett. B* **785**, 551 (2018), arXiv: 1709.00773[nucl-ex]
- [17] J. Adam *et al.* (STAR), *Phys. Rev. C* **100**, 014902 (2019), arXiv: 1903.05370[nucl-ex]
- [18] J. Adam *et al.* (STAR), *Phys. Rev. Lett.* **126**, 092301 (2021), arXiv: 2001.02852[nucl-ex]
- [19] M. Abdallah *et al.* (STAR), *Phys. Rev. C* **104**, 024902 (2021), arXiv: 2101.12413[nucl-ex]
- [20] M. Abdallah *et al.* (STAR), *Phys. Rev. Lett.* **127**, 262301 (2021), arXiv: 2105.14698[nucl-ex]
- [21] M. S. Abdallah *et al.* (STAR), *Phys. Rev. Lett.* **128**, 202303 (2022), arXiv: 2112.00240[nucl-ex]
- [22] M. Abdallah *et al.* (STAR), *Phys. Rev. C* **107**, 024908 (2023), arXiv: 2209.11940[nucl-ex]
- [23] B. Aboona *et al.* (STAR), *Phys. Rev. Lett.* **130**, 082301 (2023), arXiv: 2207.09837[nucl-ex]
- [24] M. Abdulhamid *et al.* (STAR), *Phys. Lett. B* **857**, 138966 (2024), arXiv: 2311.00934[nucl-ex]
- [25] M. Abdulhamid *et al.* (STAR), *Phys. Lett. B* **855**, 138560 (2024), arXiv: 2304.10993[nucl-ex]
- [26] J. Chen *et al.*, *Nucl. Sci. Tech.* **35**, 214 (2024), arXiv: 2407.02935[nucl-ex]
- [27] M. Abdulhamid *et al.* (STAR), (2025), arXiv: 2504.00817[nucl-ex]
- [28] J. Xu, S. Yu, F. Liu *et al.*, *Phys. Rev. C* **94**, 024901 (2016), arXiv: 1606.03900[nucl-ex]
- [29] S. A. Bass *et al.*, *Prog. Part. Nucl. Phys.* **41**, 255 (1998), arXiv: nucl-th/9803035
- [30] M. Bleicher *et al.*, *J. Phys. G* **25**, 1859 (1999), arXiv: hep-ph/9909407
- [31] X. Luo, J. Xu, B. Mohanty *et al.*, *J. Phys. G* **40**, 105104 (2013), arXiv: 1302.2332[nucl-ex]
- [32] A. Chatterjee, Y. Zhang, J. Zeng *et al.*, *Phys. Rev. C* **101**, 034902 (2020), arXiv: 1910.08004[nucl-ex]
- [33] Y. Ye, Y. Wang, J. Steinheimer *et al.*, *Phys. Rev. C* **98**, 054620 (2018)
- [34] Y. Ye, Y. Wang, Q. Li *et al.*, *Phys. Rev. C* **101**, 034915 (2020), arXiv: 2004.11745[nucl-th]
- [35] A. Chatterjee, Y. Zhang, H. Liu *et al.*, *Chin. Phys. C* **45**, 064003 (2021), arXiv: 2009.03755[nucl-ex]
- [36] M. L. Miller, K. Reygers, S. J. Sanders *et al.*, *Ann. Rev. Nucl. Part. Sci.* **57**, 205 (2007), arXiv: nucl-ex/0701025
- [37] X. Luo, *Phys. Rev. C* **91**, 034907 (2015), arXiv: 1410.3914[physics.data-an]
- [38] CBM Collaboration, *CBM progress report 2023*, (2023), accessed on 16 June 2025.
- [39] Z. Sweger (STAR Collaboration), *Proton high-order cumulants results from the star fixed-target program*, https://indico.cern.ch/event/1334113/contributions/6369534/attachments/3048338/5386843/QM2025_Sweger_v64.pdf, Quark Matter 2025, accessed April 9, 2025.